Determination of Blood Flow Parameters in a Cylindrical Vessel

Grzegorz Dwojakowski, Artur Klepaczko, Andrzej Materka
Institute of Electronics
Lodz University of Technology
Lodz, Poland
grzegorz.dwojakowski@dokt.p.lodz.pl

***Abstract* — Data from Magnetic Resonance Angiography carries information about the structure of blood vessels in the human brain. Thanks to proper segmentation methods, this information can be used in diagnosis. However, the correct assessment of these algorithms is troublesome. We have proposed a new concept of validating segmentation results. The idea is to create an MRA Simulator. The output images can then be compared with the pattern, which would not be possible using real data. This paper explains how various physical phenomena were modeled to simulate blood flow. The proper assortment of these parameters will be used to obtain images similar to those that come from the Time of Flight method.**

Keywords* — *Magnetic Resonance Imaging, image segmentation, blood vessel network, blood flow modeling

I. Introduction

Magnetic Resonance Imaging (MRI) is one of radiology techniques used to visualize the internal structure of the human body [1]. Modern MRI scanners can receive high resolution 3D images with good contrast between different tissues. In comparison to traditional X-rays or Computer Tomography, MRI is noninvasive because it does not use ionizing radiation. Another advantage is the number of different sequences. Using angiographic techniques such as Time of Flight [2] and Susceptibility Weighted Imaging [3] methods combined together, results in a full map of veins and arteries [4]. Such a map carries important information about a patient's health and can be used in diagnosis and planning surgical operations.

Anomalies, such as clots at latter stage of diseases or neoplasmic diseases, are clearly visible and can be detected by radiologists without difficulty. But is it possible to spot narrowings in small vessels and clots in early stages of diseases? Because of the high complexity of the vessel networks there is a significant risk of omitting those areas.

In these situations image segmentation and visualization methods can be useful [5][6]. Separating vessels from other tissues allows to show arteries and veins as a 3D model (Fig. 1). Data in this form is much easier to be analyzed than 2D cross-sections [7]. Additionally segmentation allows to automatically search for risk regions based on vessel diameter. As shown above, benefits of segmentation are significant.

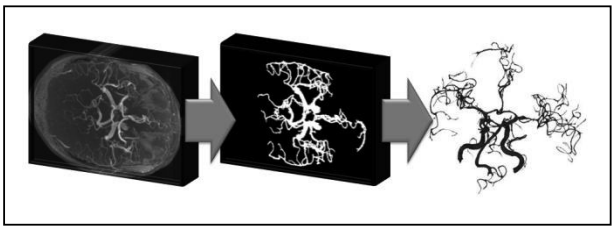

Figure 1. Results of brain vessels segmentation and visualization.

II. Validation Methods

Every image processing method, before used in a hospital, must be validated first [8][9]. It is necessary to give medical doctors a reliable tool to make correct diagnoses. How many vessels were detected? Were diameters and shapes reconstructed correctly? Were artifacts resulting from the imaging acquisition technique minimized? In order to validate the segmentation algorithm it is necessary to answer these questions.

Usually results are compared with the pattern. This time the pattern is the brain vessel network. It is not possible to properly measure such a complex structure inside a human skull. In this case, the validation process is different.

The easiest method of validation is based on a medical knowledge and subjective assessment made by doctors [10]. However, gathered information cannot be used as a reliable pattern due to uncertainty and poor reproducibility.

Second group of validation is based on physical phantoms. These artificial structures are mainly used to calibrate MRI scanners, but can also be used to test results of segmentation methods. This time, the pattern is familiar and comparison can be made. This method of validation is much more accurate, but has its drawbacks. Physical phantoms are expensive and, so far, there is no structure similar to the real blood network. This is a result of complicated topology and small vessel diameters.

The third group consists of digital phantoms [11]. Similarly to physical structures they are a familiar pattern. A complex geometrical shape is much easier to create using computer 3D graphics. What is more, they are much faster and cheaper to create. They can be duplicated with different parameters and can be used to create large set of test objects. The only disadvantage is that it is not possible to use these phantoms in a real MRI scanner.

To solve this problem, and make digital phantoms usable, we must create an MRI simulator. Using this program we should be able to obtain images similar to this from a real scanner (with noise and distortion caused by imaging sequence). A properly implemented simulator working on digital phantoms will create an effective and objective criterion of validation for image segmentation methods.

III. MRI SIMULATOR

Simulating the physical phenomena of an MRI scanner is a complex problem. Only a few attempts to this issue can be found in the literature [12][13][14][15], but they work only for invariable objects. In case of angiographic imaging, these methods cannot be used because sequences such as Time of Flight (ToF) and Susceptibility Weighted Imaging (SWI) are based on blood flow in arteries and veins. In ToF, image contrast is acquired by unsaturated molecules of blood which flows through acquisition volume in a given time moment. SWI depends on blood oxygenation and uses amplitude and phase gradient echo, with compensated blood flow effect.

As it was shown above, in order to simulate MRA sequences, there is a need to determinate fluid flow parameters in an artificial blood vessel network.

IV. MODEL SETUP:

Appropriate simulation of blood flow is a crucial issue for the whole project. Only the right model and its positive results will provide the possibility of using MRI simulator as a reliable validation tool. To determine the flow parameters we use COMSOL Multiphysics environment [16]. Results will be validated using real phantoms. After the comparing process, parameters will be ready to implement in the system.

A. Geometry

As mentioned earlier, model geometry should be identical to the physical phantom in order to perform validation. This phantom should have a familiar geometry accuracy and fluid flow must be possible in it. From among several models, we chose the Flow Phantom Set (Fig. 2) produced by Shelley Medical Imaging Technologies [17]. This Model is compatible with the high class CompuFlow 1000 MR pump [18].

This Phantom Set consists of 4 straight and 1 U-bend tubes. Diameters are between 5-8 millimeters. There is no fluid leek through the walls and no deformation caused by flow. This simplification makes the model easier to implement.

The 3D model of a simple cylinder can be constructed with COMSOL drawing Tools. To create more complex shapes including sinusoidal stenosis and bifurcations it is necessary to create geometry in the outside program. Models in this article were constructed using the Visualization Toolkit for C++ [19]. We also tested geometry created in Google Scatchup [20]. In each case, models were interpreted correctly by COMSOL.

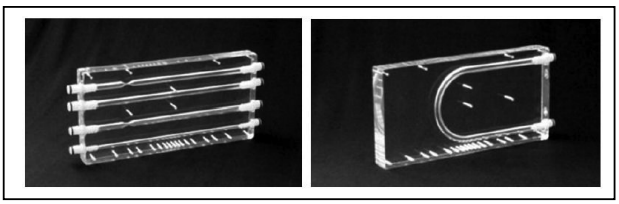

Figure 2. Phisical phantoms made of sylicon [17[. Left: Stright cylinders with stenosis. Right: U-bend tube.

B. Fluid

After creating geometry, vessels must be filled with blood. Two main parameters describing this liquid are viscosity and density. Based on literature these values were set to 1060 Kg/m^3 (density) and 0.005 Ns/m^2 (dynamic viscosity) [21]. These two parameters are sufficient to model the flow.

Blood transport in vessels is generally modeled using laminar flow equations [22]. This model assumes that fluid flows in parallel layers. Each layer has its own speed and slides past one another so there is no lateral mixing. For simulating blood flow in a pipe with ideal circular cross-section, this model is sufficient. Blood flows in one direction. Velocity is greatest in the middle of the cylinder. The value decreases as we approach the vessel wall.

Real vessels are not ideal tubes. Diameter is not a constant value. It can change gradually or rapidly in stenosis. Bifurcations are another obstacle for laminar flow; when one cylinder is divided into 2 smaller ones with different directions. In those type of situations fluid is no longer flowing in layers and turbulence appears. However, the vast majority of attempts of blood flow simulations in vessels relay on a laminar model. The main reason for this is the complexity of turbulent flow phenomenon. In this paper we modeled flow in vessel bifurcation using the laminar and turbulent model. Our goal is to compare these two results and decide if the idea of simplifying calculations is justifiable.

COMSOL Multiphysics gives possibility to simulate both types of flow. Laminar flow is generated by solving incompressible Navier-Stokes equations [23]. To simulate turbulences one of three Reynolds-averaged Navier-Stokes (RANS) model can be used [24].

A very interesting package was added to COMSOL since the 4.2a version. The name of this module is Particle Tracing [25]. Its main feature is an estimation trajectory of a chosen molecular. We have been looking forward to it since it was announced. The reason to this was the fact that information about direction and speed of blood particles is necessary to

simulate such sequences as ToF or SWI. Now the version 4.2a has been released, it can be tested and validated.

V. RESULTS

To test the described modules, we used 3 types of digital phantoms (Fig. 3). Straight cylinder, tube with stenosis and simple bifurcation model. First two were created in the likeness of the synthetic model. After positive test results, both phantoms can be compared. The third model is a brunch which divides into two smaller tubes according to the rule of bifurcation.

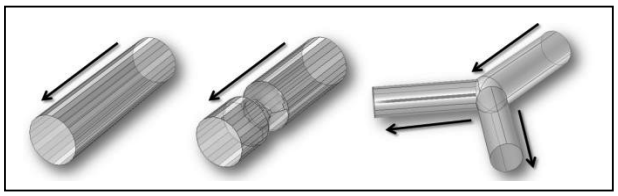

Figure 3. Three digital models. From left: Stright tube, tube with stenosis, bifurcation. Arrows indicate the direction of blood flow.

A. Straight tube

Straight tube is a perfect model to simulate Laminar flow. The geometrical shape of all orthogonal cross-sections is an ideal circle. The diameter is set to 8 mm and the length of a tube is equal to 100mm. Fluid flow is forced by setting pressure difference between input and output boundaries. There is no slip allowed through phantom walls. This assessment was made for three reasons:

- In vessels with 8mm diameter blood transfer through the wall is negligible.
- Synthetic phantom has no slip.
- It simplifies calculations.

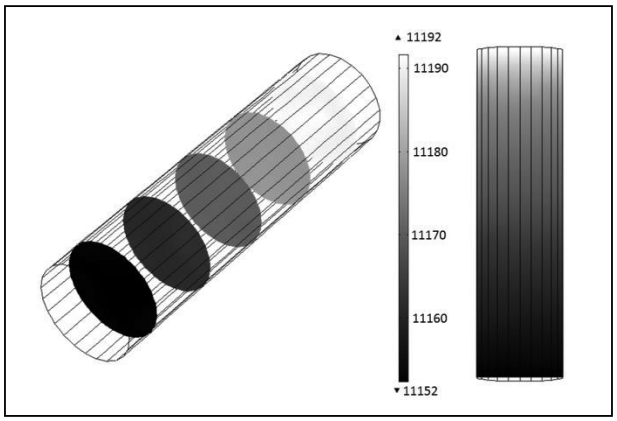

Figure 4. Preasure distribution in straight tube. Preasure range is 11.208-11.148 Pa

The results of simulation can be visible on Figure 4 and 5. According to the theory of laminar flow, highest velocity is obtained in the center of the tube (bright color). Moving towards the wall this value decreases.

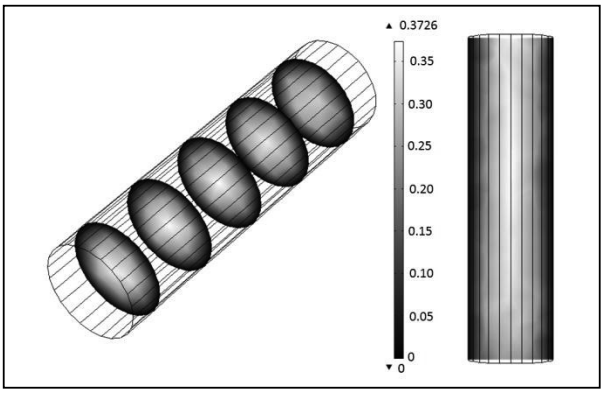

Figure 5. Velocity magnitude in straight tube. Value range is 0.0-0.37 m/s

Based on the laminar flow solution, particle tracing was performed. The Number of molecules was set to 128. All of them were defined by density and diameter. At the beginning, all particles are located at input boundary. With time, each element moves towards the exit (Fig. 7, top 3 pictures). All trajectories are straight lines parallel to the main axis of the vessel. The fastest particles reach its goal in less than one second; ones next to the wall are over five times slower. Results from this study are relevant to values obtained in laminar flow simulation. What is very important, besides getting visually attractive animations, the user is able to save 3d coordinates of all particles in chosen time steps as a spreadsheet file. There is also a possibility to analyze and process this data using output programs.

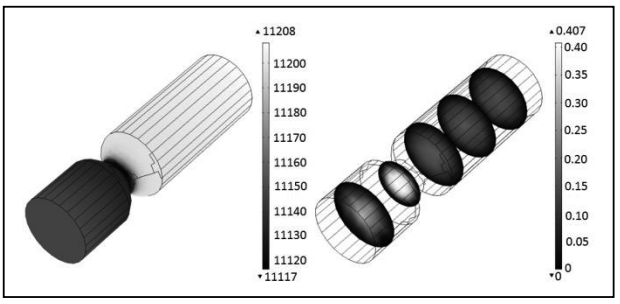

Figure 6. Tube with stenosis. Left: Preasure distribution (range is 11.208-11.148 Pa). Right: Velocity magnitude 0.0-0.43 m/s

B. Straight tube with stenosis

Another phantom created based on the synthetic model is similar 8mm diameter tube but with 50% sinusoidal stenosis by diameter. Parameters of the flow are the same as at the first test. Due to this narrowing, pressure distribution is not so linear as in the first test (Fig. 6). This time, pressure force applied on the particle before reaching stenosis is almost constant and it equals the input parameter. The pressure changes rapidly and reaches output value. In these conditions, velocity values are also different. For the first straight tube the

fastest particles have constant speed over 0.35 m/s. They reach the goal in less than 0.1 s. For cylinder with sinusoidal narrowing, the velocity value changes between the input and the output. Through the first half of the tube particles in the middle will not reach 0.20 m/s. In the region of a stenosis they double their speed for a while to slow down once again. Time of the flow is almost twice as long. After the narrowing, the density of particles is higher because they do not return to their previous positions (Fig. 7).

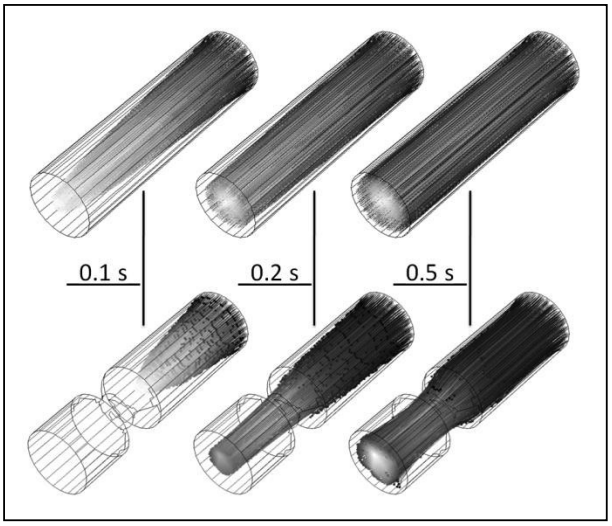

Figure 7. Particle tracing for two phanthoms with the same length and diameter.

C. *Bifurcation model*

The third phantom consists of 3 tubes: the one with the largest diameter is called the ancestor branch, the other two – descendent branches with smaller radius based on bifurcation rule. The center point of a base is common for all tubes. the deviation angle for both descendent branches is identical. In this way a simple bifurcation model was created with one input and two outputs. For this object two types of flow were implemented.

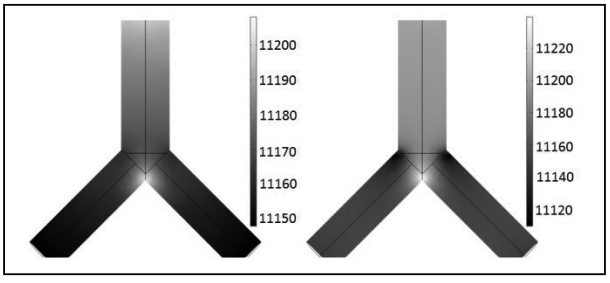

Figure 8. Preasure distribution in bifurcation model. Left: Laminar flow (range 11.208-11.148 Pa). Right: Turbulent flow (range 11.239-11.111 Pa).

For laminar flow, pressure distribution is linear (Fig. 8, left picture), similarly to the first phantom. the Velocity magnitude values are also consistent with the theory. In the ancestor branch, the direction of the velocity field is in line with the y axis. After ramification, this direction consists of two component vectors(x and y). These components have the same absolute values for both descendent brunches (Fig. 9, left picture).

Pressure and velocity values for turbulent flow are different from those obtained using the laminar model. Pressure distribution changes rapidly in the center of bifurcation. Velocity values are no longer dependant on the distance from the center of a container. In the descendent branches, blood flows according to the law of inertia, along centre walls.

For the both models particle tracking analysis was performed (Fig. 10). Trajectories from laminar flow in the ancestor branch are similar to that in straight tubes but due to different pressure at the end they move slightly towards the central axis. After bifurcation, particles travels in both tubes in the middle of the vessel. This flow is no longer laminar; velocity direction is different for every particle.

Trajectories obtained from the turbulent model of flow can be seen at figure 10. At first, all molecules have the same speed and direction. After dividing them into two groups particles move in a disorderly way.

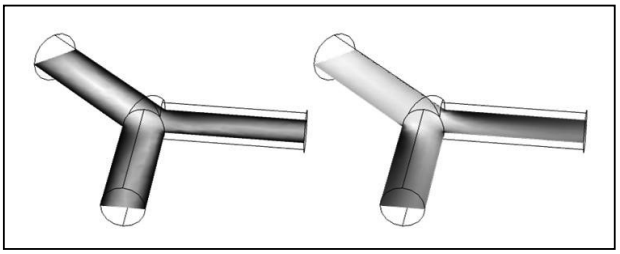

Figure 9. Velocity magnitude in bifurcation model. Left: Laminar flow (range 0.0-0.32 m/s). Right: Turbulent flow (range 0.0-0.44 m/s).

VI. PROBLEMS

Results are satisfactory and the obtained data is useful, however, there are a few problems. In our case we want to trace all particles from the beginning to the end with short timeframes (39 us). For phantoms with 10 cm length or more, it takes almost 5 seconds for all molecules to reach output. If we divide that value by timeframes, we obtain over 25.000. Each moment consists of x,y,z coordinates for all 128 particles. In result, huge amount of data is generated which is difficult to compute even by modern computers. Also the COMSOL interface was not created to handle big datasets and widgets simply stop working. The only way to deal with this situation is to divide created study into few smaller ones and connect them outside the COMSOL.

There is also a problem with the trajectory of particles near vessel walls. If a single molecule travels close enough to the edge of a cylinder, its velocity is inherited from the boundary wall. This value is 0, so the examined particle stops at one point. It happened only when input geometry was read from

the output file and cylinder orientation wasn't set along the main axis. The reason lies in limited mapping accuracy for rounded objects.

The Final problem is associated with the interpretation of results. Values obtained in the descendent branches in bifurcation model raise our concerns. There is a need to simulate these phenomena using other tools and compare results.

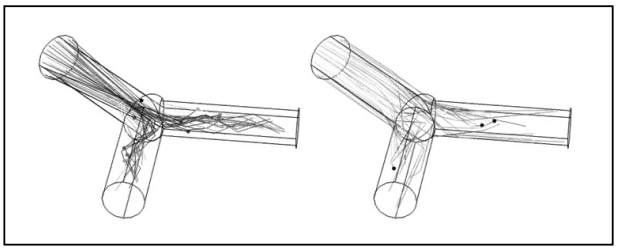

Figure 10. Particle tracing based on Laminar (left) and Turbulent model (right).

VII. CONCLUSION:

The goal of this paper was to carry out a simulation of blood flow in selected tubular objects. This task was successfully completed. Two types of flow were tested in different digital models. Expected values were obtained. Based on these simulations particle tracing was performed. 3D coordinates in time for each molecule was gathered. These values will be used in an MRI simulator to produce images similar to ToF. Due to the fact that Particle Tracing is a new module, several limitations and errors were found during the project. We proposed a way to deal with them.

ACKNOWLEDGMENT

This work was supported by the Polish National Science Centre grant no. 6509/B/T02/2011/40.

REFERENCES

[1] P. Bogorodzki, "Obrazowanie czynności mózgu techniką rezonansu magnetycznego", Przegląd Elektrotechniczny, 2009, no.9, pp. 40-45.

[2] M. A. Bernstein, J. Huston , C. Lin , G. F. Gibbs, J. P.Felmlee, "High-resolution intracranial and cervical MRA at 3.0T: technical considerations and initial experience", Magn Reson Med, 46/2001, no.5, pp. 955-962.

[3] J. R. Reichenbach, E. M. Haacke, "High resolution BOLD venographic imaging: A window into brain function, NMR Biomed, 14/2001, vol. 7-8, pp. 453-467.

[4] A. Deistung, E. Dittrich, J. Sedlacik, A. Rauscher, J. Reichenbach, "ToF-SWI Simultaneous time of flight and fully flow compensated susceptibility weighted imaging", Journal of Magnetic Resonance Imaging, 29/2009, no.6, pp. 1478-1484.

[5] C. Kirbas, F. Quek, "A review of vessel extraction techniques and algorithms", ACM Computing Surveys, 36/2004, no.2, pp. 81-121.

[6] M. Nałęcz, Tom 8 – „Obrazowanie biomedyczne", Akademicka oficyna wydawnicza EXIT(2003), Biocybernetyka inżynieria biomedyczna, 2000, vol. 8, pp. 351-372.

[7] M. Strzelecki, A. Materka, M. Kociński, P. Szczypiński, Deistung A., Reichenbach J., „Ocena metody zbiorów poziomicowych w zastosowaniu do segmentacji trójwymiarowych obrazów fantomów cyfrowych oraz obrazów naczyń krwionośnych mózgu ToF-SWI rezonansu magnetycznego", InżynieriaBiomedyczna, Acta Bio-Optica et Informatica Medica,16 /2010 , pp. 167-172.

[8] P. Jonnin, E. Krupinski, S. Warfield, „Validation in Medical Image Processing", IEEE Transactions on Medical Images, vol. 25, 11/2006, pp. 1405-1409.

[9] W. R. Crum, O. Camara, L. Derk, G. Hill, "Generalized Overlap Measures for Evaluation and Validation in Medical Image Analysis", IEEE Transactions on Medical Images, vol. 25, 11/2006, pp. 1451-1461.

[10] F. Javier Sanchez Castro, "A Cross Validation Study of Deep Brain Stimulation Targeting: From Experts to Atlas-Based, Segmentation-Based and Automatic Registration Algorithms", vol. 25, 11/2006, pp. 1440-1448.

[11] B. Aubert-Broche, M.Griffin, G. Bruce Pike, A. C. Evans, D. L. Collins, "Twenty New Digital Brain Phantoms for Creation of Validation Image Data Bases" vol. 25, 11/2006, pp. 1410-1416.

[12] H. Benoit-Cattin, G. Collowet, B. Belaroussi, H. Saint-Jalmes, C. Odet. "The simri project: a versatile and interactive MRI simulator", Journal of Magnetic Resonance, no.173(1), 2005, pp. 97–115.

[13] K. Jurczuk, M. Kretowski, "Virtual magnetic resonance imaging - parallel implementation in a cluster computing environment",. Biocybernetics and Biomedical Engineering, 29(3), 2009, pp. 31–46.

[14] R.K.-S. Kwan, A.C. Evans, G.B. Pike, "MRI simulation-based evaluation of image-processing and classification methods", Medical Imaging, IEEE Transactions on, 18(11), 1999, pp. 1085–1097.

[15] J.S. Petersson, J.O. Christoffersson, K. Golman, "MRI simulation using the k-space formalism", Magnetic Resonance Imaging, 11(4), 1993, pp. 557–568.

[16] COMSOL Multiphysics, "Realease Notes", COMSOL, COMSOL 4.1 edition, 2010.

[17] Shelley Medical Imaging Technologies,"MRI Quality Assurance Flow Phantom Set", www.simutec.com

[18] Shelley Medical Imaging Technologies,"CardioFlow 1000 MR Computer Controlled Flow System", www.simutec.com

[19] W. Schroeder, K. Martin, B. Lorensen, „The Visualization Toolkit", Prentice Hall PTR, 1998.

[20] Google, "Google SketchUp 8", http://www.sketchup.google.com/

[21] K. Cieślicki "Hydrodynamiczne uwarunkowania krążenia mózgowego", Medycyna Informatyczna, Warszawa 2001, pp. 123-190.

[22] K. Jeżowiecka-Kabsch, H.Szewczyk, „Mechanika płynów", Wrocław 2001, pp. 163-245.

[23] COMSOL Multiphysics, "Sloved with COMSOL Multiphysics 4.1", COMSOL, COMSOL 4.1 edition, 2010.

[24] M Szydłowski, P. Zima 'Two-Dimensional Vertical Reynolds-Averaged Navier-Stokes Equations Versus One-Dimensional Saint-Venant Model for Rapidly Varied Open Channel Water Flow Modeling", Archives of Hydro-Engineering and Environmental Mechanics, 53(4), 2006, pp. 295-309

[25] COMSOL Multiphysics, "Chemical Engineering Module – User's Guide", COMSOL, COMSOL 4.1 edition, 2010.